ChemComm

Accepted Manuscript

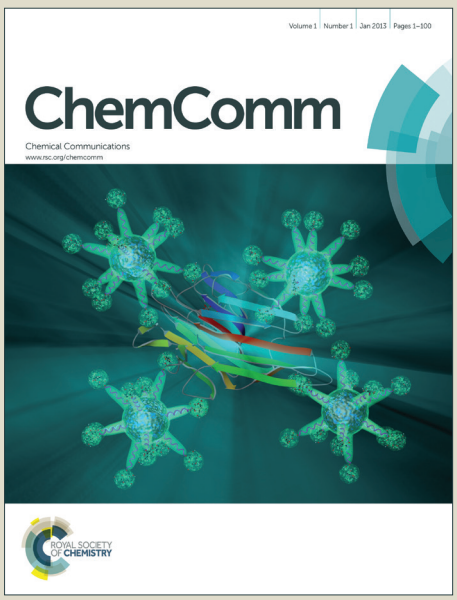

ROYAL SOCIETY OF CHEMISTRY

www.rsc.org/chemcomm

Journal Name

RSCPublishing

COMMUNICATION

Tuning the reactivity of nanostructured indium tin oxide electrodes toward chemisorption

Cite this: DOI: 10.1039/xoxxoooooox

A. Forget,[a] R. T. Tucker,[b] M. J. Brett,[b,c] B. Limoges*[,a] and V. Balland*[,a]

Received ooth January 2012,
Accepted ooth January 2012

DOI: 10.1039/xoxxoooooox

www.rsc.org/

This contribution highlights correlation between the surface concentration of a chemisorbed organophosphorous probe (Flavin mononucleotide) and the relative hydroxyl surface coverage of nanostructured ITO electrodes, which can be tuned during post-deposition reductive annealing. The resulting modified electrodes are very stable in aqueous solution, highly hydrophilic and fully-accessible to the bulk solution.

Transparent nanostructured electrodes based on doped-metal oxides such as tin-doped indium oxide (ITO) are characterized by both a high electrical conductivity and an accessible high surface area. They allow for increased conductive pathways throughout photoactive layers in organic photovoltaic devices[1–3] as well as for immobilization of large amounts of functional molecules in solar cell applications,[4] (bio-)electroanalytical devices or electrocatalytic reactors.[5–7] Besides these (bio-)technological applications, they also offer new perspectives in the development of innovative spectroelectrochemical methodologies to address some fundamental questions in the field of charge transfer reactions at solid/liquid interfaces.[7] In many studies involving such functionalized nanostructured ITO electrodes, modification of the metal-oxide surface is mainly achieved by passive physisorption of organic dyes[8] or metallo-peptides or –proteins.[5,9–11] The stability of the resulting modified electrodes is rather poor and significant desorption occurs, especially under high ionic strength experimental conditions.[7] It appears thus necessary to develop appropriate surface functionalization procedures of nanostructured ITO surfaces leading to much more stable monolayers of functional molecules. This can be achieved by transposing the surface functionalization methodologies initially developed for bulk crystalline ITO substrates[12] to nanostructured ITO surfaces. This is typically what we proposed in the present work with the surface functionalization of nanostructured ITO electrodes prepared by glancing angle deposition (GLAD). To achieve this goal, we have taken advantage of a procedure recently developed by us to form stable monolayers of chemisorbed organophosphorous compounds on bulk ITO surfaces under mild conditions.[13]

3D ITO electrodes suitable for the above-mentioned applications require preparation of thick nanostructured films deposited onto a transparent and usually conductive glass substrate. This can be achieved by different processes leading to various film morphologies. Recently, nanostructured ITO electrodes were obtained either chemically using sol-gel processes[4,5,8] and controlled self-assembly of nanoparticles,[14] or physically through the sintering of ITO nanoparticles coating, dc-sputtering[15] and by vacuum-based glancing-angle deposition (GLAD).[16] In most of these processes, metal oxide deposition is followed by annealing steps to improve the physical properties of the material, including stability, transparency and conductivity. An air annealing step is notably required to calcinate the organic template and crystallize the metal-oxide nanoparticles in chemical processes,[4,8] or to improve the transparency of GLAD-ITO films.[17] An additional annealing step performed under N_2 or H_2-based forming gas is also usually necessary to optimize the 3D ITO film conductivity by increasing the concentration of free charge carriers resulting from oxygen vacancies.[8,14,17,18] These additional annealing steps have been shown to strongly modify the surface chemical composition of ITO,[19] potentially thus affecting the chemisorption reactivity of functional molecules bearing organophosphorus moieties. One purpose of the present paper was to analyze the influence of the reductive annealing step on the surface reactivity of GLAD ITO electrodes. This latter technique allows for preparation of nanostructured ITO films which shape, porosity and thickness that can be easily controlled and tuned during the deposition step.[3,7,16] To characterize the surface reactivity of these nanostructured ITO electrodes towards organophosphorous compounds, we have used the redox-active flavin mononucleotide (FMN) molecule. This molecule was previously shown to strongly chemisorb on bulk ITO surface through its phosphate anchoring group, a surface reaction that could be easily electrochemically monitored through the redox-active properties of the chemisorbed compound. It was also previously found that the FMN surface coverage on bulk ITO was quite sensitive to the surface hydroxyl content.[13] Another interest in using this redox probe is that it exhibits a strong dependence to local pH changes,[20] a property that can be leveraged for examining whether the nanostructured electrode provides a specific local environment to the chemisorbed molecules as well as a restricted accessibility to the solvent.

One micrometer thick porous GLAD-ITO electrodes were prepared on ITO-coated glass substrates using a deposition angle of 75° as already described in literature.[9,16] The resulting

nanostructured electrodes exhibit vertical columnar structures of ITO grains (Figure 1), with areal column density and column diameter variation along the film depth. After deposition, a first annealing step was performed under air to enhance the transparency of the film in the visible range. GLAD-ITO electrodes were then submitted to a second annealing step for 1 hour at 375 °C under forming gas (H_2/N_2 5:95) by using various gas flow rates (ranging from 10 to 300 sccm, see SI for details). This reductive treatment is known to increase the material conductivity by decomposition of the top oxygen layer.[17,19] The resulting oxygen loss of the ITO surface was indeed evidenced by the decrease of the O/(In+Sn) ratio determined from XPS analysis of the ITO surface (Figure S1).[19] We noticed concomitantly a decrease in the ITO film transmittance, down to complete loss of transparency for films submitted to high forming gas flow rates (i.e. 300 sccm) (Figure 1, Table S1). The GLAD-ITO electrodes were also systematically characterized by cyclic voltammetry (45 mM Hepes, 320 mM KCl, pH 7.25, T = 20°C). We have observed no significant change in either the magnitude of the capacitive current density or in the residual ohmic drop whatever the reductive annealing treatment of the GLAD-ITO electrode.

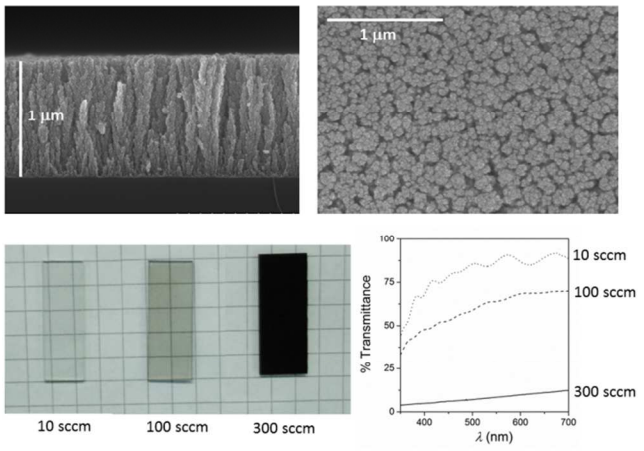

Figure 1: Top: Side- and top-view of the 1 µm GLAD-ITO film obtained by scanning electron microscopy. Below: Transparency of the GLAD-ITO electrodes after reductive annealing in forming gas at 10, 100 and 300 sccm.

Prior functionalization, GLAD-ITO electrodes were chemically cleaned from organic contaminants by soaking in different solvents (see SI for details). Functionalization was then achieved by soaking the cleaned electrodes in a 100 µM FMN solution in aqueous media at pH~5 for 20 hours. According to the high affinity of the FMN for ITO, these experimental conditions ensure surface coating saturation. The resulting FMN-GLAD-ITO electrodes were then soaked in a buffer solution at 50°C to desorb low affinity fractions of adsorbed FMN. Immediately after rinsing, the modified electrodes were characterized by cyclic voltammetry in a FMN-free buffer solution, and the resulting integrated faradaic anodic or cathodic peak current then used to determine the FMN surface coverage (assuming a 2 e^- transfer reaction) as a function of time immersed in the FMN solution. A typical cyclic voltammogram (CV) is reported in Figure 2A. It is characterized by a well-resolved symmetrical faradaic wave centered at a midpoint potential value of -0.45 V (*vs.* SCE) for all modified electrodes (Table S1). The variation of FMN surface coverage as a function of the time in the electrochemical cell is reported in Figure S2. As previously reported for dense ITO electrodes, two fractions of adsorbed FMN could be identified. The first one, characterized by a slow desorption rate of ca. 4 h^{-1}, is attributed to strongly physisorbed FMN molecules, mainly through a combination of hydrogen bonds and electrostatic interactions. The second one much more resistant to desorption is attributed to a chemisorbed fraction characterized by a surface concentration Γ_χ ranging from 0.1 to 4.15 nmol cm^{-2}, depending on the GLAD-ITO reductive annealing treatment (Table S1). The high stability of this chemisorbed fraction is evidenced by the fact that 65-70 % still remains adsorbed after 7 days soaking in the aqueous buffer solution.

The CV corresponding to this chemisorbed FMN fraction on a 100 sccm GLAD-ITO electrode (Γ_χ = 3.3 nmol.cm^{-2}) is given in Figure 2A and is characterized by a ΔE_p value of 35 mV and fwhm value of 110 mV at 0.1 V s^{-1}. This latter value significantly differs from the theoretical value of 45 mV expected for a 2 e^- transfer redox process. Such non ideality was previously reported with flavin-modified electrodes.[21–23] It may result from inhomogeneities in the adsorbate populations and/or surface binding sites, or from unfavorable lateral interactions between the adsorbed FMN molecules.

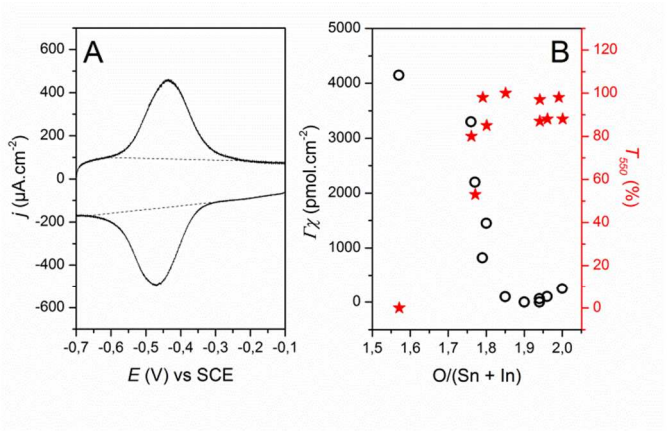

Figure 2. A: CV of a modified FMN-GLAD-ITO electrode (100 sccm, O/(Sn+In)=1.76) recorded after 24 hours of desorption (scan rate 0.1 V.s^{-1}, 45 mM Hepes, 320 mM KCl, pH 7.25, T = 20°C). B: (○) surface concentration of the FMN chemisorbed fraction Γ_χ and (★) transmittance monitored at 550 nm of the GLAD-ITO electrodes prepared under various reductive annealing conditions, plotted as a function of the surface oxygen atomic ratio determined from XPS.

Plotting Γ_χ values as a function of the O/(Sn+In) ratio of GLAD-ITO electrodes clearly evidences a strong correlation with the ITO oxygen surface content (Figure 2B). Chemisorption of phosphate moieties appears indeed to be highly favored on GLAD-ITO electrodes having low surface oxygen content. This observation is fully consistent with a chemisorption mechanism involving first a nucleophilic addition of the negatively charged FMN phosphate oxygen on an acidic (i.e. oxygen deficient) surface metal site as previously suggested for dense ITO electrodes.[13] Moreover, we assume that this adsorption process is concomitant with a slow ITO surface hydroxylation, leading to a progressive standardization of the GLAD-ITO electrodes surface hydroxyl density. This may explain why the chemisorbed FMN midpoint potential, reflecting potential interactions with the local metal-oxide environment, is almost independent of the initial ITO surface oxygen content. The highest surface coverage Γ_χ of 4.15 nmol cm^{-2} is obtained with the most reduced GLAD-ITO electrode (300 sccm, O/(Sn+In)=1.57). Once corrected from the 60-fold surface enhancement of the GLAD-ITO electrode, this value (ie., 68 pmol cm^{-2}) is in agreement to the one previously obtained (ie., 76 pmol cm^{-2}) at commercial bulk ITO electrodes characterized by an O/(Sn+In) ratio of 1.62 and functionalized under similar experimental conditions (Table S1).[13] It

remains however low as compared to the theoretical saturating FMN surface concentration of 0.5 nmol cm^{-2} calculated for a close-packed monolayer on a flat surface.[24] We assume thus that FMN chemisorption on ITO is limited by the number of metal oxide sites exhibiting high Lewis acidity. The similar values reported for the 300 sccm GLAD-ITO and the commercial flat ITO electrodes confirm that the surface chemical composition is the main factor governing chemisorption.

It is worth to note that even though these highly reduced electrodes show better chemisorption properties; their lack of transparency hinders applications in the field of optoelectronic devices. The best compromise between transparency and reactivity was achieved with GLAD-ITO electrodes prepared under a 100 sccm forming gas flow rate and characterized by an O/(Sn+In) ratio of 1.75-1.80. Although the surface coverage of the chemisorbed molecules remains low as compared to the theoretical surface saturation, it can still be easily detected by UV-visible absorption spectroscopy (Figure S4), preserving thus the possibility to couple electrochemical methods with spectroscopies.

Thereafter, we analyzed the dependence of the apparent reduction potential of the chemisorbed FMN to pH-changes in the bulk solution. Accordingly, FMN-GLAD-ITO electrodes (100 sccm) were left to desorb in a Hepes buffer for 24 hours prior characterization by cyclic voltammetry in a mixture of buffer (see SI) and at low scan rates (in order to ensure thermodynamic equilibrium). The modified GLAD-ITO electrodes showed quite good stability for pH ranging from 4 to 9, but significant desorption at pH > 9 (Figure S3). The midpoint potential $E_{m,pH}$ of the chemisorbed FMN was reported as function of pH (Figure 3) and the resulting experimental plot fitted to the following equation:[20]

$$E_{m,pH} = E_{m,0} + 2.303\frac{RT}{2F}\log\left(\frac{[H^+]^3 + K_{a,red}[H^+]^2}{[H^+] + K_{a,ox}}\right) \qquad (1)$$

where $E_{m,0}$ is the FMN apparent reduction potential corresponding to the two one-electron reduction transitions at pH 0, R = 8.314 J K^{-1}, T is the temperature (20 °C), F is the faradaic constant (96500 C mol^{-1}) and $K_{a,red}$ and $K_{a,ox}$ refer to the protonation constant of the oxidized and fully reduced FMN.

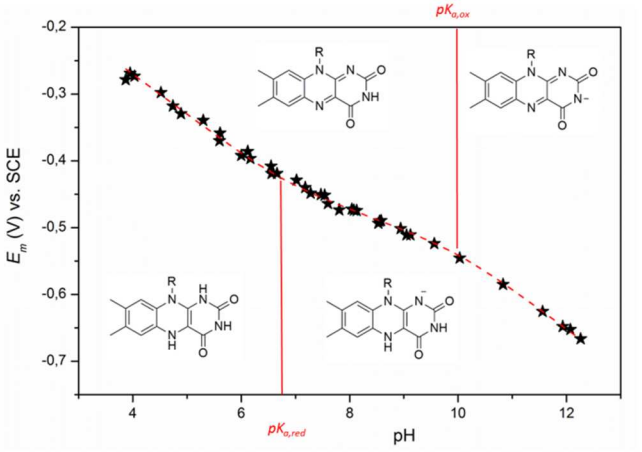

Figure 3. Potential-pH diagram of FMN chemisorbed in GLAD-ITO electrodes (100 sccm) obtained with two distinct electrodes. Experimental midpoint potential values (★) and fitting (----) according to eq 1 with $E_{m,0}$ = -0.03 V *vs.* SCE, $K_{a,red}$ = 1.8 x 10^{-7}, $K_{a,ox}$ = 9.2 x 10^{-11}.

From the best fit to the experimental data, the following parameters were inferred: $E_{m,0}$ = -0.03 V (*vs.* SCE), $pK_{a,ox}$ = 10.0, and $pK_{a,red}$ = 6.75. These values are very similar to those reported for the free FMN in solution ($E_{m,0}$ = -0.04 V, $pK_{a,ox}$ = 10.3 , $pK_{a,red}$ = 6.8),[20] clearly demonstrating that both redox as well as acid-base equilibria of the chemisorbed FMN are almost unaffected by the vicinity of the metal oxide surface. This result strongly differs from that obtained with other conductive surfaces such as flavin-modified gold or carbon electrodes for which the midpoint potentials pH-dependence of the adsorbed flavins were observed significantly affected by the hydrophobic microenvironment of the electrode, as well as by the nature and chemical composition of surface (for instance, the presence of an hydrophobic self-assembled monolayer).[22,24–26] It confirms thus indirectly the high hydrophilicity of ITO surfaces. Our results also evidence that the chemisorbed FMN remains highly sensitive to pH changes in the bulk solution, demonstrating the high accessibility of the GLAD-ITO pores to the buffer solution.

In conclusion, we demonstrate that efficient chemisorption of organophosphorous molecules within nanostructured ITO electrodes can be achieved under mild conditions, preserving the nanostructured metal oxide network. We highlight the crucial role of the post-deposition reductive annealing step on the reactivity of the metal oxide: the higher the network of ITO is reduced the more reactive it behaves with respect to the FMN chemisorption in aqueous solution. We evidence moreover that the redox- and pH-properties of the FMN molecule are unaffected by chemisorption. This study demonstrates that mesoporous GLAD-ITO electrodes characterized by a well-opened porosity are suitable for the preparation of modified electrodes requiring full-accessibility. It thus paves the way for the preparation of highly stable nanostructured electrodes modified by functional molecules for applications in solar cells, (bio-)electroanalytical devices or electrocatalytic reactors.

Notes and references

[a] Laboratoire d'Electrochimie Moléculaire, UMR CNRS 7591, Université Paris Diderot, Sorbonne Paris Cité, 15 rue Jean-Antoine de Baïf, F-75205 Paris Cedex 13, France. *E-mail : limoges@univ-paris-diderot.fr; veronique.balland@univ-paris-diderot.fr

[b] Electrical and Computer Engineering, University of Alberta, Edmonton, Alberta, Canada T6G 2V4.

[c] NRC National Institute for Nanotechnology, Edmonton, Alberta, Canada T6G 2M9.

Electronic Supplementary Information (ESI) available: Material and Methods, O(1s) XPS spectra of GLAD-ITO electrodes, desorption kinetics of FMN-GLAD-ITO electrodes, cyclic voltamograms of FMN-GLAD-ITO electrodes at various pH. See DOI: 10.1039/c000000x/

1. F. Yang and S. R. Forrest, *ACS Nano*, 2008, **2**, 1022–1032.
2. M. K. Fung, Y. C. Sun, A. Ng, A. M. C. Ng, A. B. Djurišić, H. T. Chan, and W. K. Chan, *ACS Appl. Mater. Interfaces*, 2011, **3**, 522–527.
3. A. L. Beaudry, R. T. Tucker, J. M. LaForge, M. T. Taschuk, and M. J. Brett, *Nanotechnology*, 2012, **23**, 105608.
4. W. Hamd, M. Chavarot-Kerlidou, J. Fize, G. Muller, A. Leyris, M. Matheron, E. Courtin, M. Fontecave, C. Sanchez, V. Artero, and C. Laberty-Robert, *J. Mater. Chem. A*, 2013, **1**, 8217–8225.
5. S. Frasca, T. von Graberg, J.-J. Feng, A. Thomas, B. M. Smarsly, I. M. Weidinger, F. W. Scheller, P. Hildebrandt, and U. Wollenberger, *ChemCatChem*, 2010, **2**, 839–845.
6. Y. Aksu, S. Frasca, U. Wollenberger, M. Driess, and A. Thomas, *Chem. Mater.*, 2011, **23**, 1798–1804.
7. C. Renault, C. P. Andrieux, R. T. Tucker, M. J. Brett, V. Balland, and B. Limoges, *J. Am. Chem. Soc.*, 2012, **134**, 6834–45.
8. D. Fattakhova-Rohlfing, T. Brezesinski, J. Rathouský, a. Feldhoff, T. Oekermann, M. Wark, and B. M. Smarsly, *Adv. Mater.*, 2006, **18**, 2980–2983.

9. C. Renault, K. D. Harris, M. J. Brett, V. Balland, and B. Limoges, *Chem. Commun.*, 2011, **47**, 1863–1865.
10. R. Vitale, L. Lista, S. Lau-Truong, R. T. Tucker, M. J. Brett, B. Limoges, V. Pavone, A. Lombardi, and V. Balland, *Chem. Commun.*, 2014, **50**, 1894–1896.
11. D. Schaming, C. Renault, R. T. Tucker, S. Lau-Truong, J. Aubard, M. J. Brett, V. Balland, and B. Limoges, *Langmuir*, 2012, **28**, 14065–72.
12. P. J. Hotchkiss, S. C. Jones, S. A. Paniagua, A. Sharma, B. Kippelen, N. R. Armstrong, and S. R. Marder, *Acc. Chem. Res.*, 2012, **45**, 337–346.
13. A. Forget, B. Limoges, and V. Balland, *Langmuir*, 2015, **31**, 1931–1940.
14. Y. Liu, G. Štefanić, J. Rathouský, O. Hayden, T. Bein, and D. Fattakhova-Rohlfing, *Chem. Sci.*, 2012, **3**, 2367.
15. M. K. Fung, Y. C. Sun, a. M. C. Ng, X. Y. Chen, K. K. Wong, a. B. Djurišić, and W. K. Chan, *Appl. Phys. A*, 2011, **104**, 1075–1080.
16. K. M. Krause, M. T. Taschuk, K. D. Harris, D. a Rider, N. G. Wakefield, J. C. Sit, J. M. Buriak, M. Thommes, and M. J. Brett, *Langmuir*, 2010, **26**, 4368–76.
17. D. A. Rider, R. T. Tucker, B. J. Worfolk, K. M. Krause, A. Lalany, M. J. Brett, J. M. Buriak, and K. D. Harris, *Nanotechnology*, 2011, **22**, 085706.
18. T. Von Graberg, P. Hartmann, A. Rein, S. Gross, B. Seelandt, C. Röger, R. Zieba, A. Traut, M. Wark, J. Janek, and B. M. Smarsly, *Sci. Technol. Adv. Mater.*, 2011, **12**, 025005.
19. R. X. Wang, C. D. Beling, S. Fung, a. B. Djurišić, C. C. Ling, and S. Li, *J. Appl. Phys.*, 2005, **97**, 033504.
20. S. G. Mayhew, *Eur. J. Biochem.*, 1999, **265**, 698–702.
21. J. Liu, M. Paddon-Row, and J. Gooding, *J. Phys. Chem. B*, 2004, **0**, 8460–8466.
22. J. M. Goran and K. J. Stevenson, *Langmuir*, 2013, **29**, 13605–13.
23. J. M. Goran, S. M. Mantilla, and K. J. Stevenson, *Anal. Chem.*, 2013, **85**, 1571–81.
24. S. Tam-Chang, J. Mason, I. Iverson, K.-O. Hwang, and C. Leonard, *Chem. Commun.*, 1999, 65–66.
25. E. E. J. Calvo, M. S. Rothacher, C. Bonazzola, I. R. Wheeldon, R. C. Salvarezza, M. E. Vela, and G. Benitez, *Langmuir*, 2005, **21**, 7907–7911.
26. G. Nöll, E. Kozma, R. Grandori, and J. Carey, *Langmuir*, 2006, 2378–2383.

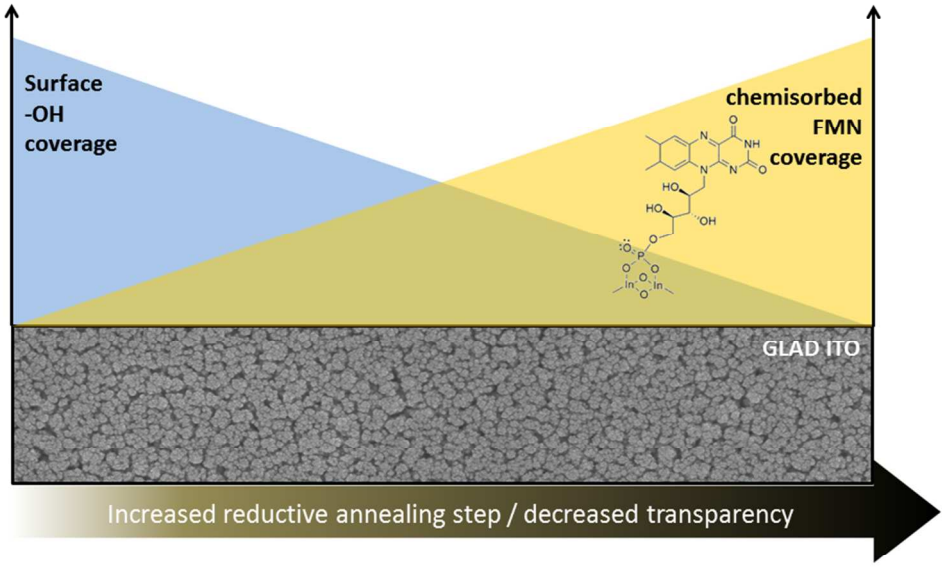

254x190mm (96 x 96 DPI)